Enhanced plasticity of Zr-based bulk metallic glass matrix composite with ductile reinforcement

Y.F. Sun
Research Center for Materials, Department of Materials Science and Engineering, Zhengzhou University, Zhengzhou 450002, People's Republic of China; and National Microgravity Lab, Institute of Mechanics, Chinese Academy of Sciences, Beijing 10080, People's Republic of China

B.C. Wei, Y.R. Wang, and W.H. Li
National Microgravity Lab, Institute of Mechanics, Chinese Academy of Sciences, Beijing 10080, People's Republic of China

C.H. Shek[a)]
Department of Physics and Materials Science, City University of Hong Kong, Hong Kong

(Received 27 January 2005; accepted 26 April 2005)

A composite material containing uniformly distributed micrometer-sized Nb particles in a Zr-based amorphous matrix was prepared by suction cast. The resulting material exhibits high fractured strength over 1550 MPa and enhanced plastic strain of about 29.7% before failure in uniaxial compression test at room temperature. Studies of the serrations on the stress–strain curves and the shear bands on the fractured samples reveal that the amplitude of the stress drop of each serration step corresponds to the extent of the propagation of a single shear band through the materials. The composite exhibits more serration steps and smaller amplitude of stress drop due to the pinning of shear band propagation by ductile Nb particles.

I. INTRODUCTION

Recently, extensive investigations have been done in the development of bulk metallic glass (BMG) matrix composites. Attempts are made to improve the plasticity of the monolithic BMG, which typically display limited plastic strain of 0–2% in compression and nearly zero in tension at room temperature due to the highly localized shear bands.[1–5] For example, some Zr-based BMG matrix composites containing micrometer-sized ductile crystalline phases such as body-centered-cubic (bcc) structured β dendrite or refractory metals, e.g., Nb, Ta, and W, exhibit combinations of the high strength of the amorphous matrix and the high ductility of the reinforcement. The achievements greatly expand the potential application of BMGs.[6–10] The reinforcement in the composite material is known to resist the propagation of the highly localized shear bands effectively and promote the generation of multiple shear bands. Delayed failure and improved toughness of the materials result. However, the interaction of the reinforcement and the shear bands is still not very clear. Greer et al.[11] and Chen et al.[12] proposed that nanocrystalline particles with the scale comparable with the thickness of the shear bands could influence the development of the shear bands. However, Hays et al.[10] and Kühn et al.[13] believed that particles with a mean size close to the width of the shear bands have little effect in stopping its propagation. In any case, the interaction between the shear bands and the second phase can be reflected by the shear bands characterization on the fractured plane and the serrated flow variation during the compression test or nanoindentation test. For example, Wei et al. proposed that a change from the serrated flow for monolithic BMGs to continuous flow for Nb-based BMG composites would occur.[14]

In this paper, we report the preparation and the mechanical properties of a composite material with an amorphous matrix reinforced by micrometer-sized particles of Nb, which are added to the $Zr_{65}Al_{10}Ni_{10}Cu_{15}$ alloy melt prior to casting. The composite material shows not only high yield strength but also apparent strain hardening and very large plastic deformation of about 29.7% before failure in uniaxial compression at room temperature. The mechanism of the enhanced plastic deformation is discussed in the light of the serration characterizations on the stress–strain curves and the shear bands pattern on the fractured samples.

$Zr_{65}Al_{10}Ni_{10}Cu_{15}$ alloy was used as a matrix material for the composite. Ingots weighing approximately 30 g of the matrix alloy were prepared by arc melting a mixture

[a)]Address all correspondence to this author.
e-mail: apchshek@cityu.edu.hk
DOI: 10.1557/JMR.2005.0320

of the constitutive elements of purities above 99.5%. Nb was selected as the reinforcement because of its excellent ductility with the largest elongation up to about 30%. About 3 g Nb powder with particle size of about 15 μm were dispersed in the molten matrix alloy by remelting the ingot at a temperature a little higher than the melting point. Seventy-millimeter-long samples with 3-mm diameter were then suction cast into a water cooled copper mold under Ti-gettered argon atmosphere. Slices of the composite rod were examined by a Siemens D 500/501 X-ray diffractometer with Cu K_α radiation for phase identification. Thermal analysis of the as-cast composites was carried out using differential scanning calorimetry (DSC) at a continuous heating rate of 0.33 K/s. Uniaxial compression tests were performed at an initial strain rate of 1×10^{-4} s^{-1} with an Instron 5562 testing machine, which has an axial stiffness of 100 kN/mm and a strain measurement accuracy of 0.05% of full scale and 0.5% of reading. The compression specimens were 6 mm long and 3 mm in diameter with the ends polished to ensure parallelism. A JEOL JSM 5200 scanning electron microscope (SEM) was used for microscopic fractography of the fractured specimen.

The microstructure of the as-cast composites is shown in Fig. 1. Circular particles with an average size of about 15 μm are dispersed throughout the amorphous matrix. It reveals that the Nb is not dissolved substantially into the amorphous matrix during the melting process due to its high melting temperature of 2742 K. Energy dispersive spectroscopy (EDS) measurements show that the matrix contains about 2 at.% Nb. The x-ray diffraction (XRD) pattern inset in Fig. 1 was taken from the cross section of the as-cast composite. The sharp diffraction peaks from Nb element can be observed superimposing on a broad diffraction halo, which is the typical feature of amorphous phase.

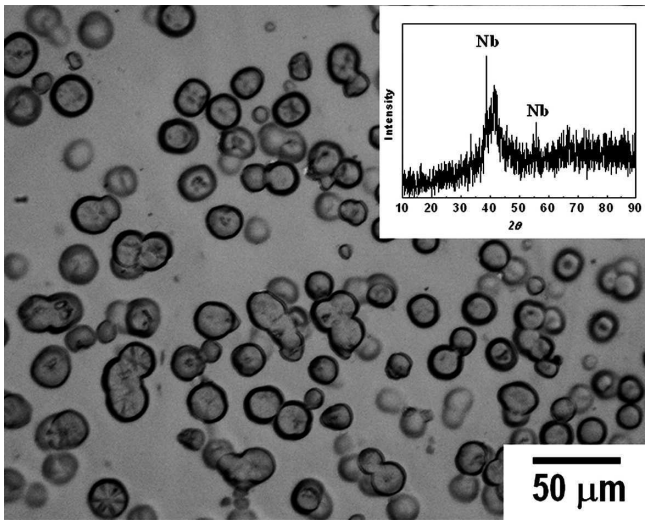

FIG. 1. Optical micrograph and XRD pattern of the as-cast composites.

Figure 2 shows the DSC curves of the as-cast Nb-reinforced composite and the monolithic BMG. Both curves exhibit an obvious glass transition at temperature T_g, followed by one exothermic reaction with the onset temperature T_x. The T_g and T_x of the composites shift to a value a little higher than that of the monolithic BMG. However, the supercooled liquid regions $\Delta T = T_x - T_g$ of the two samples are nearly the same. The crystallization enthalpy ΔH of the composites is less than that of the BMG. This difference may be due to the lower volume fraction of amorphous phase in the composite. Table I lists the T_g, T_x, ΔT, and ΔH of the Nb-reinforced composites and the monolithic BMG.

A series of room temperature compression tests were conducted on the Nb-reinforced $Zr_{65}Al_{10}Ni_{10}Cu_{15}$ BMG matrix composites and the as-cast monolithic BMG. In each case, the samples were tested to failure. Figure 3(a) shows the engineering stress–strain curves of the two samples. Both samples show linear elasticity up to the elastic limit followed by yielding and plastic strain. The Young's modulus (E) of the composites is about 92.1 GPa, which is a little less than the value of 97.4 GPa of the BMG. After reaching the elastic limit, the monolithic BMG starts yielding with an ultimate strength of 1947 MPa. This is followed by a strain-softening stage, which often occurs in BMGs due to the structural change of the material in the shear bands, leading to a local

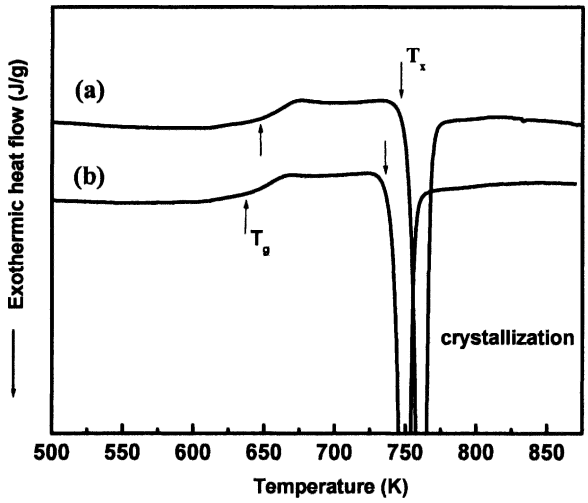

FIG. 2. DSC data collected from the composite and monolithic BMG at a heating rate of 20 K/min: (a) Nb-reinforced composite and (b) monolithic BMG.

TABLE I. T_g, T_x, ΔT, and ΔH of the Nb-reinforced composites and the monolithic BMG.

Samples	T_g (K)	T_x (K)	ΔT (K)	ΔH (J/g)
BMG composite	646	747	101	97
BMG	637	736	99	85

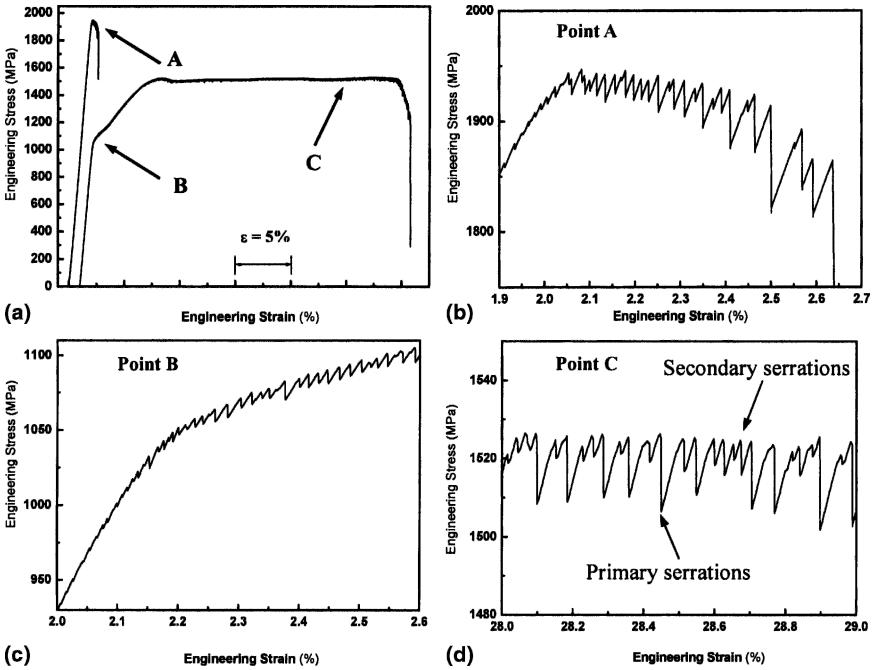

FIG. 3. Compressive stress–strain curves for as-cast Nb-reinforced composite and its corresponding monolithic BMG loaded to failure: (a) complete curves of both samples and (b, c, d) detailed serrated pattern for points A, B, and C in (a).

lowering of the viscosity.[15] The total strain of the monolithic BMG is about 2%. The composite yields at a lower stress of about 1050 MPa, followed by obvious work hardening and significant plastic strain with ultimate fracture strength of about 1550 MPa. The total strain of the composites is about 29.7%, which is one of the best ductility for BMG matrix composites developed so far.

Detailed study of the stress–strain curves of both samples reveal that serrated flow occurs immediately after yielding. However, the serration features on the stress–strain curves of the two samples are quite different. To shed light on the difference of the serration features, portions of the stress–strain curves in Fig. 3(a) are shown in Figs. 3(b)–3(d) at higher magnification. For monolithic BMG, the number of serrations steps on the curves is relatively small, and the stress drop, defined as the stress change from the highest to the lowest points of each serration step, increases with time and hence with strain. The amplitude of the last stress drop can reach about 100 MPa. However, for Nb-reinforced composites, the stress drop of each serration step remains more or less constant and with amplitude of no more than 20 MPa. The number of the serration is much more than that of monolithic BMG. Upon closer inspection, there are two kinds of serrations on the curves of the composite as indicated by arrows and labels in Fig. 3(d). One is the primary serrations with stress drop of about 20 MPa and another kind is secondary serration with stress drop of about 5 MPa. These two kinds of serrations appear on the stress–strain curves successively and several secondary serrations occur between two single primary serrations. The relationship of the serrations with the shear bands will be discussed in the following.

Figure 4 presents the SEM micrographs showing fractography of the samples after being compressed to failure. For Nb-reinforced composites, multiple shear bands form due to the branching of individual shear bands as they propagate through the material. Slip steps on the lateral surface of the composites shown in Fig. 4(a) are much more jagged and typically occur as groups of several slip steps cluster together. It is suggested that the shear bands parallel to the fracture plane are considered as primary shear bands, and the others are considered as branched shear bands. Multiple shear bands can be observed on the lateral surface near the fracture plane, as well as far away from the fracture plane, indicated by arrows and labels in Fig. 4(b). Figure 4(c) shows the fractured plane of the composites, while the shear bands on the lateral surface can also be seen. On the fractured plane, fractured Nb particles can be found embedded in the matrix as indicated by a white arrow. The inset image in Fig. 4(c) shows some dimples on the fractured plane, and they might be caused by Nb particles peeling off from the matrix. For monolithic BMG shown in Fig. 4(d), only a few shear bands can be observed at an angle of about 45° with respect to the stress axis and parallel to the fracture plane.

In the present condition, it is suggested that the ductile Nb particle plays a crucial role for dramatically enhanced plasticity. When the stress reaches the yield point under

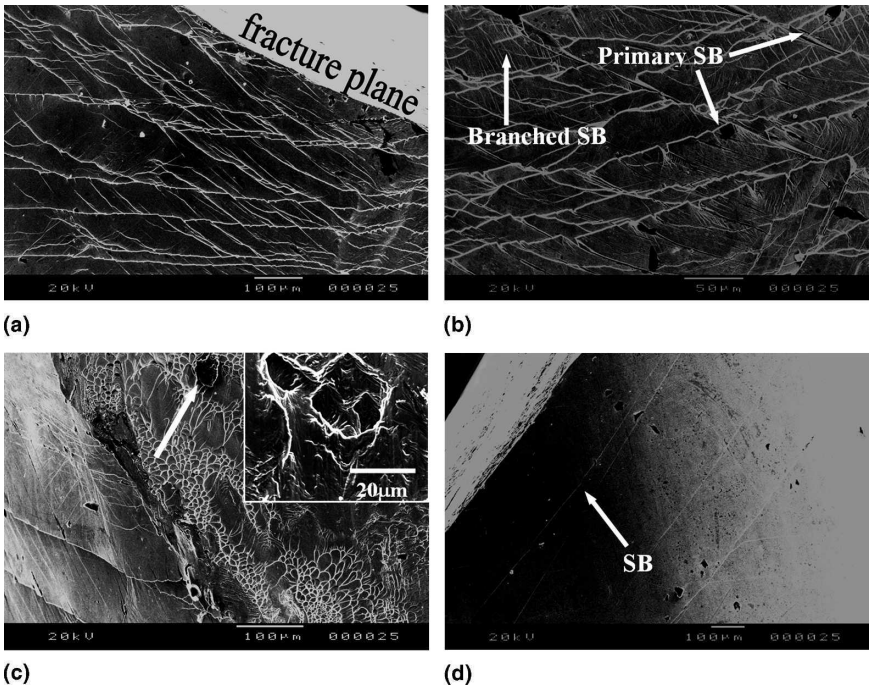

FIG. 4. Fractography of the specimen compressed to failure at room temperature: (a, b, c) Nb-reinforced composite and (d) monolithic BMG.

loading, the Nb particles will yield at first during compression and contribute to the strain-hardening via dislocation multiplication. Due to the larger volume fraction in the composite, the matrix must carry a larger portion of the load. When the matrix reaches its elastic limit, shear bands are generated and propagate, resulting in the plastic deformation of the sample. After loading increased to a certain extent, some Nb particles will fracture because of its tight interfacial bonding with the matrix. The remaining Nb particles still contribute to strain-hardening. On the other hand, the concurrent generation of the shear bands in the glassy matrix will lead to strain-softening, which will lead to stress drop. The strain-hardening contributed by the Nb particles is just sufficient to counteract the stain-softening in the glassy matrix in this case and resulted in a relatively smooth stress–strain curve. Since the plastic deformation achieved by BMGs is confined almost entirely in narrow regions near the shear bands, the extent of plastic deformation in BMG is largely dependent on the density of the shear band. As for the BMG matrix composites, the second phase in the BMG matrix increases the resistance for the propagation of shear bands, resulting in extensive branching of the shear bands.[16] Therefore, the composite resists failure either by arresting the propagation of shear bands or branching into secondary shear bands. The branching can distribute the plastic strains associated with the shear band, and the shear strain in any one branch may be much smaller than that of a single, unbranched shear band. This makes it more difficult for a propagating shear band to result in a crack cutting through the whole cross section, and therefore the plastic strain prior to failure is increased.

It is widely accepted that each serration on the stress–strain curves correspond to the nucleation of single shear bands. Therefore, the study of the serration can help understand the shear band development under loading. Previous study of the serrated flow on the stress–strain curves indicates that the stress drop of one serration depend strongly on the strain rate, temperature, and material microstructure. Justin et al.[17] suggested that the amplitude of the stress drop would decrease with increasing strain rate, which is similar to the serrated flow variations in some BMG alloys under nanoindentation test. Pink et al. suggested that the stress drop in single serration is sensitive to changes in the microstructure and has been shown to be closely related to the formation of Guinier-Preston (GP) zones and precipitates in $AlZn_5Mg$ and Al–Zn–Mg–Cu alloys.[18–20] In crystalline alloys, the stress drop variations correspond to the interaction of dislocation and the solute while in BMGs, the stress drops are proposed to correspond to the nucleation and development of shear bands. Comparing the serration variations on the stress–strain curves and the shear band structure on the lateral surfaces of the fractured samples, we propose that the amplitude of the stress drop of each serration corresponds to the extent of the shear bands propagation through the samples under loading. The smaller stress drop in a single serration means a larger resistance for a shear bands to propagate through the material. The shear bands will branch to comply with the macroscopic shape change. As for monolithic BMG, the

shear bands nucleate after yielding and propagate simply through the materials. The resultant stress drop is large, indicating large extent of single shear band propagation. For the Nb-reinforced composites, the primary serrations with the stress drop of about 20 MPa in Fig. 3(d) is suggested to correspond to the nucleation and development of the primary shear band. The secondary serration with the stress drop of about 5 MPa in Fig. 3(d) should correspond to the nucleation and development of the branched shear bands. The serrations in Fig. 3(d) therefore confirm that the shear band will separate into several branches when the primary shear bands are pinned by the Nb particles. This agrees well with the shear bands characterization in Figs. 4(a) and 4(b).

In conclusion, the Nb-reinforced $Zr_{65}Al_{10}Ni_{10}Cu_{15}$ BMG matrix composite deforms more homogeneously, showing obvious strain hardening, and exhibits significant plastic deformation before failure, with the total strain of about 29.7%. The serration features on the stress–strain curves are quite different from that of the corresponding monolithic BMG. For the composites, the number of the serrations is large but the stress drop of each serration is significantly smaller than that of the monolithic BMG. It is suggested that the amplitude of the stress drop of each serration correspond to the extent of the shear band propagation through the materials. The shear band propagation would be pinned by the Nb-particles and will branch into multiple shear bands, which distribute the stress more homogeneously and results in great plastic deformation.

ACKNOWLEDGMENTS

This work was supported by a City University of Hong Kong Strategic Research Grant (Project No. 7001529), Knowledge Innovation Program of Chinese Academy of Sciences (Project No. KJCX2-SW-L05), and National Natural Science Foundation of China (Grant No. 50101012).

REFERENCES

1. H. Choi-Yim and W.L. Johnson: Bulk metallic glass matrix composites. *Appl. Phys. Lett.* **71,** 3808 (1997).
2. C. Fan, D.V. Louzguine, C.F. Li, and A. Inoue: Nanocrystalline composites with high strength obtained in Zr–Ti–Ni–Cu–Al bulk amorphous alloys. *Appl. Phys. Lett.* **75,** 341 (1999).
3. R.D. Conner, R.B. Dandliker, and W.L. Johnson: Mechanical properties of tungsten and steel fiber reinforced $Zr_{41.25}Ti_{13.75}Cu_{12.5}Ni_{10}Be_{22.5}$ metallic glass matrix composites. *Acta Mater.* **46,** 6089 (1998).
4. C.P. Kim, R. Busch, A. Masubr, H. Choi-Yim, and W.L. Johnson: Processing of carbon-fiber-reinforced $Zr_{41.2}Ti_{13.8}Cu_{12.5}Ni_{10.0}Be_{22.5}$ bulk metallic glass composites. *Appl. Phys. Lett.* **79,** 1456 (2001).
5. Z. Bian, M.X. Pan, Y. Zhang, and W.H. Wang: Carbon-nanotube-reinforced $Zr_{52.5}Cu_{17.9}Ni_{14.6}Al_{10}Ti_5$ bulk metallic glass composites. *Appl. Phys. Lett.* **81,** 4740 (2002).
6. H. Choi-Yim, R.D. Conner, F. Szuecs, and W.L. Johnson: Processing, microstructure and properties of ductile metal particulate reinforced $Zr_{57}Nb_5Al_{10}Cu_{15.4}Ni_{12.6}$ bulk metallic glass composites. *Acta Mater.* **50,** 2737 (2002).
7. U. Kühn, J. Eckert, N. Mattern, and L. Schultz: ZrNbCuNiAl bulk metallic glass matrix composites containing dendritec bcc phase precipitates. *Appl. Phys. Lett.* **80,** 2478 (2002).
8. Q.L. Dai, B.B. Sun, and M.L. Sui: High-performance bulk Ti–Cu–Ni–Sn–Ta nanocomposites based on a dendrite-eutectic microstructure. *J. Mater. Res.* **19,** 2557 (2004).
9. G. He, J. Eckert, W. Löser, and L. Schultz: Novel Ti-base nanostructure-dendrite-composite with enhanced plasticity. *Nat. Mater.* **2,** 33 (2003).
10. C.C. Hays, C.P. Kim, and W.L. Johnson: Microstructure controlled shear band pattern formation and enhanced plasticity of bulk metallic glasses containing *in situ* formed ductile phase dendrite dispersions. *Phys. Rev. Lett.* **84,** 2901 (2000).
11. A.L. Greer, A. Castellero, S.V. Madge, I.T. Walker, and J.R. Wilde: Nanoindentation studies of shear banding in fully amorphous and partially devitrified metallic alloys. *Mater. Sci. Eng.* **375–577,** 1182 (2004).
12. M.W. Chen, A. Inoue, and C. Fan: Fracture behavior of a nanocrystallized $Zr_{65}Cu_{15}Al_{10}Pd_{10}$ metallic glass. *Appl. Phys. Lett.* **74,** 2131 (1999).
13. U. Kühn, J. Eckert, N. Mattern, and L. Schultz: Microstructure and mechanical properties of slowly cooled Zr–Nb–Cu–Ni–Al composites with ductile bcc phase. *Mater. Sci. Eng. A* **375–377,** 322 (2004).
14. B.C. Wei, T.H. Zhang, and W.H. Li: Serrated plastic flow during nanoindentation in Nd-based bulk metallic glasses. *Intermetallics* **12,** 1239 (2004).
15. F. Spaepen: A microscopic mechanism for steady state in homogeneous flow in metallic glasses. *Acta Metall.* **25,** 407 (1977).
16. T.C. Hufnagel, F.R. Cang, and T. Ott: Controlling shear band behavior in metallic glasses through microstructural design. *Intermetallics* **10,** 1163 (2002).
17. J.M. Reed and M.E. Walter: Observation of serration characteristics and acoustic emission during serrated flow of an Al–Mg alloy. *Mater. Sci. Eng.* **A359,** 1 (2003).
18. E. Pink: The effect of precipitates on characteristics of serrated flow in $AlZn_5Mg_1$. *Acta Metall.* **37,** 1773 (1989).
19. A. Deschamps, M. Niewczas, and F. Bley: Low-temperature dynamic precipitation in a supersaturated Al–Zn–Mg alloy and related strain hardening. *Philos. Mag. A* **79,** 2485 (1999).
20. D. Thevenet, M. Mliha-Touati, and A. Zeghloul: The effect of precipitation on the Portevin–Le Chatelier effect in an Al–Zn–Mg–Cu alloy. *Mater. Sci. Eng. A* **266,** 175 (1999).